Journal of Polymer Research (2019) 26: 136
https://doi.org/10.1007/s10965-019-1798-1

ORIGINAL PAPER

Shape memory hydroxypropyl cellulose-*g*-poly (ε-caprolactone) networks with controlled drug release capabilities

Marzieh Jahangiri[1] · Alireza Evazzadeh Kalajahi[2] · Mostafa Rezaei[2] · Massoumeh Bagheri[1]

Received: 21 August 2018 / Accepted: 25 April 2019 / Published online: 12 May 2019

Abstract

Hydroxypropyl cellulose-*g*-poly (ε-caprolactone) (HPC-*g*-PCL) derived networks from different lengths of PCL side chains have been prepared by crosslinking HPC-*g*-PCL, providing (X(HPC-*g*-PCL)) films with different gel contents, crystallinity, and morphology. Two networks with different ε-cCaprolactone (CL) content (95 and 98%) named X(HPC-*g*-PCL)-95 and X(HPC-*g*-PCL)-98 were used for further study of thermo-mechanical properties and shape memory behavior. Young's modulus (E), elongation at break (ε_b %) and tensile strength (σ_m) were examined at three different temperatures 22, 37 and 65 °C. The results revealed that E values significantly were controlled by crystallinity as well as crosslink density depending on the temperatures. Complete shape recovery was observed for both samples once the degree of crosslinking was increased over 95%, while a narrower recovery temperature ranges from 39 to 41 °C was found for the X(HPC-*g*-PCL)-98 sample. The shape fixity results showed a great dependence on the molecular weight of PCL. Therefore, the X (HPC-*g*-PCL)-98 sample demonstrated an excellent shape fixation. Naproxen-loaded shape memory films prepared using either the in situ (before crosslinking) or swelling (after crosslinking) methods (3 and 10 wt%), were also described as a model for controlled drug release device. The chemical composition of drug-loaded networks, drug concentration and the incorporation method greatly affected the crosslink density, morphology and mechanical properties. Importantly, loading via the in situ method resulted possibility to adjust the amount of incorporated drug and fast subsequent release, while drug-loaded films by the swelling method exhibited an initial burst release. Both networks exhibited slow sustained release of naproxen over two months.

Keywords Poly(ε-caprolactone) · Hydroxypropyl cellulose · Mechanical properties · Shape memory polymer · Thermoresponsive · Drug release

Introduction

Stimuli-responsive polymers (SRPs) are smart materials which can show noticeable changes in their properties by environmental stimulus variations [1]. Shape memory polymers (SMPs) are an interesting class of SRPs, which have attracted great concern due to their specific properties and potential applications in various fields from biomedicine to aerospace [2]. SMPs can be deformed and fixed into a stable predefined temporary shape and have the capability to recover their original permanent shape under an external stimulus such as temperature [3], light [4], pH [5], moisture [6], chemicals [7], electrical or magnetic field changes [8, 9]. While, the shape memory effect can be activated electronically, magnetically, or electromagnetically, the most common shape memory trigger is thermal activation. Thermo-responsive SMPs are stimuli-sensitive materials whose shape is modulated by heat [7]. In general, thermally induced SMPs are considered to consist of molecular switches and net-points [10, 11]. The net-points can be either physically or chemically cross-linked structures. The latter usually shows higher mechanical strengths due to stronger interactions between the polymer chains. The switching segments determine the switching temperature, which needs to be exceeded to induce the temporary shape and recover the permanent shape when cycled through their thermal transition

Electronic supplementary material The online version of this article (https://doi.org/10.1007/s10965-019-1798-1) contains supplementary material, which is available to authorized users.

✉ Massoumeh Bagheri
massoumehbagheri@yahoo.com

[1] Chemistry Department, Science Faculty, Azarbaijan Shahid Madani University, P.O. Box: 53714-161, Tabriz 5375171379, Iran

[2] Polymer Engineering Faculty, Sahand University of Technology, 5331711111, New Town of Sahand, Tabriz, Iran

temperature (T_{trans}) [12]. T_{trans} typically may be either glass transition temperature (T_g) or melting point temperature (T_m). However, T_m is preferred due to a sharper transition and better shape recovery [13]. From biomedical point of view, combination of shape memory effect and the good biocompatibility of polymers has led to SMPs which is mostly interested for biomedical applications such as drug delivery, biosensors and biomedical devices, and implant materials [2, 14, 15]. Examples of such devices include stents [16, 17], heart valves, and septal defect occluder [15, 18]. Improvement of the degradable SMPs such as implant materials due to their minimally invasive surgery as well as no need for second surgery to remove implant materials is highly regarded [19, 20]. Various types of biodegradable SMPs based on poly(DL-lactide) (PLA) and poly(ε-caprolactone) (PCL) have been prepared for the development of smart implant devices [21]. The SMPs consist of PCL are of particular interest in biomedical applications due to their biocompatibility, biodegradability, elasticity, sharp and tunable T_{trans}, high shape recoverability, high shape fixity ratios and good mechanical properties [22–24]. Thus, PCL-based SMPs have been widely studied and prepared as both physically and chemically crosslinked networks. Some methods have been reported to modify the T_m of PCL to the body temperature [25], which adjusting the average molecular weight (M_n) of PCL chains and designing the branch structure for PCL are the most popular methods. In addition to biodegradability, thermally induced SMPs indicated the potential for use as intelligent materials in controlled drug delivery systems [15, 17, 21, 26]. Neffe et al. prepared a crosslinked SMPs by UV-curing of oligo[(ε-caprolactone)-co-glycolide]-dimethacrylates. Then, Ethacridine lactate (EL) and Enoxacin (EN) were incorporated into the polymer matrix. The influence of incorporation of drugs on the shape memory functionality, biodegradation of the SMP network on drug diffusion, as well as the programming process and shape recovery on drug release were studied [12, 15, 17]. Nagahama et al. developed a new branched architecture SMPs based on chemically crosslinking of branched oligo(ε-caprolactone) precursors with hexamethylene diisocyanate (HDI) in the presence of theophylline. The resulted polymer network, exhibited good sustained drug releasing in 35 days with remarkable temperature sensitivity and shape recovery in a narrow temperature range from 37 to 39 °C [15, 17, 27]. Also, the SMP network of star shape amorphous copolyester urethane was prepared by Wiscke et al. The resulting polymer demonstrated a controlled release of the loaded drug without losing its SMP properties in 80 days [17, 21, 28]. Recently, Serrano et al. reported a new class of crosslinked shape memory elastomers with capability of eluting drugs based on citric acid and dioles [17, 29].

We are interested in preparing new biocompatible and biodegradable PCL-based SMPs with switching temperature around body temperature. We have also developed drug-eluting SMPs to develop controlled release devices for minimally invasive surgery systems. Although, a few multifunctional polymers with shape-memory effect, biodegradability and controlled drug release have been developed, our research strategy for the development of such a multifunctional polymer system was based on used methods of the incorporation of drug molecule to affect the shape memory functionality and drug release profile. Hence, in our previous work [30], hydroxypropyl cellulose (HPC), a nontoxic, biodegradable, and biocompatible cellulose derivative, was used as a multifunctional initiator for grafting PCL in different reaction conditions. The grafted samples were crosslinked by HDI and subsequently the process was optimized by the response surface methodology (RSM). HPC was essential to reduce the PCL degree of crystalinity, therefore, a reduced T_m for PCL could be observed for prepolymers (HPC-*g*-PCL) and chemically crosslinked polymeric networks. The synthesized polymer networks based on PCL and HPC (X(HPC-*g*-PCL)) had adjustable T_{trans} ranging from 32 to 53 °C.

In the present study, we have developed SMPs comprising PCL and HPC with excellent shape fixing capability and mechanical properties. They also have demonstrated good shape recovery properties and their T_{trans} are slightly above the body temperature (39–41 °C). Naproxen is a propionic acid derivative and a non-steroidal anti-inflammatory drug (NSAID) with anti-inflammatory, antipyretic and analgesic activities and as a model drug was incorporated into the polymer matrix by two different methods. In situ drug incorporation method allows the crosslinking of HPC-*g*-PCL films in the presence of drug. In the swelling method the drug loads after the crosslinking step. So, the main objective of this article is to investigate the thermal and mechanical properties and shape memory behavior of cross-linked HPC-*g*-PCL polymers before and after drug incorporation. Furthermore, drug release behaviors from the drug-loaded films were studied. The chemical structure of the HPC-*g*-PCL polymers and networks were characterized using ^{1}H NMR spectroscopy, differential scanning calorimetry (DSC), X-ray diffraction (XRD), tensile test, and shape memory programming processes.

Experimental section

Materials

Hydroxypropyl cellulose (HPC) was purchased from Aldrich (Milwaukee, WI, USA; M_n = 100,000 gmol^{-1} according to the manufacturer) and dried under vacuum at room temperature for 24 h before use. The molar substitution of propoxy groups (MS_{HPC}) was approximated 1.25 using ^{1}H NMR spectrum of HPC [31]. ε-Caprolactone (CL) was purchased from Merck (Germany) and dried over freshly powdered CaH_2 for 24 h and then purified by twice distillation process under reduced

pressure. Tin (II) bis (2-ethylhexanoate) ($Sn(Oct)_2$, 96%) was purchased from Alfa Acer. Hexamethylene diisocyanate (HDI) was provided from Fluka and used without any further purification. Naproxen was purchased from Pharmacia and recrystallized in ethanol and distilled water for three times. Chloroform and toluene were dried by heating over sodium with benzophenone as indicator and freshly distillated before use. Tetrahydrofuran and n-hexane were used as received.

Synthesis procedure

Synthesis of HPC-*g*-PCL polymers

The synthesis procedure of the HPC-*g*-PCL prepolymers were detailed in our previous article (Scheme S1, Supporting Information) [30]. The preparation method of the HPC-*g*-PCL-98 (with 98%wt. of CL) is described as a representative case. Thus, HPC and CL at 2:98 weight ratio were added into a dry flask and the mixture was slowly stirred at room temperature for 24 h until HPC was completely swelled by CL. Then, the swelled mixture was placed in an oil bath at 130 °C under argon atmosphere. Then 1.25% (*w/w*) of $Sn(Oct)_2$ to CL was dissolved in dry toluene (0.05 g/mL) and added into the mixture. The resulted mixture was stirred for 24 h at the same temperature. In order to remove PCL homopolymer as the main by-product, the obtained polymer was dissolved in THF at a concentration of 5% (*w/v*). It was precipitated subsequently in equal volume of cold n-hexane. The purification procedure was repeated three times and the pure grafted polymer was dried overnight to yield branched HPC-*g*-PCL-98 prepolymer [31].

Preparation of X(HPC-*g*-PCL) networks

Shape memory films were previously prepared in our laboratory by crosslinking a series of HPC-*g*-PCL prepolymers having different chain lengths of PCL graft with different quantities of HDI through two different routes [30]. In this work, SMP films of PCL with thickness about 300 μm were prepared by dissolving 1 g of prepolymer in 15 mL of anhydrous $CHCl_3$. As a homogenous viscose solution was obtained, 15% (*v/w*) HDI was added as a cross-linker. The mixture was molded into a Teflon dish and dried at room temperature for 24 h. Then, the casted film was cured in an oven at 80 °C for another 24 h (Route II in our previous work) [30] to obtain X(HPC-*g*-PCL)-N networks (N is related to the weight content of CL in samples).

Preparation of drug- loaded X(HPC-*g*-PCL) films

As a model drug, naproxen was incorporated into the polymer network by two different methods.

In situ *method of drug-loading* was conducted by dissolving two different amounts of naproxen (3.0 and 10.0%wt.) in a chloroform based solution of prepolymer. The solutions were stirred for 30 min. The resulted drug/polymer mixtures were subjected to crosslinking to obtain X(HPC-*g*-PCL)-N/P% (In situ) (N and P are related to the weight content of CL and weight percent of dissolving drug in samples).

Swelling method of drug-loading was directed by immersing the dry polymer networks in a 100-fold excess (*v/w*) of a saturated drug solution in chloroform for 24 h with subsequent drying the drug-loaded films at reduced pressure to obtain X(HPC-*g*-PCL)-N/P% (Swelling). The amount of incorporated naproxen was quantified by acidic methanolysis of the polymer network. Then, the concentration of extracted naproxen was determined by UV spectroscopy as described by Neff et.al. [12].

Characterization techniques

The swelling ratio (Q) and gel content (G) of X(HPC-*g*-PCL) networks were determined to evaluate the cross-linking degree of grafted polymer networks [32, 33]. For this purpose, samples were cut into small slices and weighted carefully (m_o). After swelling in chloroform for 48 h at room temperature, the swollen extracted specimens were weighted again (m_s). Extracted samples were dried at ambient temperature until constant weight was achieved and the final weight (m_d) was recorded. Q and G were calculated according to the following equations:

$$Q = 1 + \frac{\rho_1}{\rho_2}\left(\frac{m_s}{m_d} - 1\right)$$

$$G = \left(\frac{m_d}{m_o}\right)$$

Where ρ_1 and ρ_2 are the swelling medium and polymer specific density, respectively. ρ_2 was measured using a pycnometer [33].

FT-IR spectra were recorded on a Brucker PS-15 spectrometer (Bruker Optics, Ettlingen, Germany) at wave numbers ranging from 400 to 4000 cm^{-1}. ^1H NMR spectra of the HPC-*g*-PCL polymers were recorded using a ^1H NMR spectrometer (400 MHz Brucker SP-400 Avance spectrometernsile Bruker Biospin, Rheinstetten, Germany) using chloroform as solvent and tetramethylsilane as the internal standard. The enthalpy change (ΔH_m), melting temperature (T_m) and degree of crystallinity (X_c) of the PCL prepolymer and their corresponding cross-linked films were measured by differential scanning calorimetry (type DSC 822 from Mettler-Toledo, Switzerland) under nitrogen purge from 0 to 100 °C at a heating rate of 10 °C/min in three cycles (first heating, first cooling and second heating) [30]. The crystalline structure of the polymer films was analyzed using X-ray diffraction (XRD) patterns by a Bruker

AXS model D8 advanced diffractometer for Cu Kα radiation (λ = 1.54187 Å) at 40 kV and 35 mA with Bragg angle ranging from 3 to 70°. The microstructures of the crosslinked samples, before and after drug incorporating were examined on a VEGA\\TESCAN-XMU scanning electron microscope (SEM). The samples were sputter-coated with gold prior to SEM observation and the examination voltage and magnification level were 10.0 kV and 10,000×, respectively. Mechanical properties of the polymer networks (dumbbell shape specimen, according to ISO 527-2 (type 5B)) was determined in an elongation rate of 5 mm/min at 22, 37 and 60 °C using a tensile test machine (type Z010 from Zwick/Roell, Germany) equipped with 10KN load cell [27, 34–36]. The shape-memory behaviors of the X(HPC-*g*-PCL) networks were investigated by cyclic tensile thermo-mechanical tests in a tensile testing machine (type Z010 from Zwick/Roell, Germany) [19, 36]. To examine the shape memory effect, the samples were heated to 65 °C for 10 min and stretched from permanent shape to temporary shape with an elongation rate of 5 mm/min, and hold for 10 min (ε_m). The aforementioned test was conducted for at least three specimens and was repeated three times. This temporary shape was fixed by cooling the sample to 20 ± 2 °C with the same ε_m. Subsequently, after unloading the samples and measuring their length (ε_u), the temperature increased up to T_m and kept again for 10 min to recover the original shape (ε_p). Finally, the shape fixity (R_f) and the shape recovery (R_r) were calculated according to the following equations [13, 27, 32, 37]:

$$R_f = \frac{\varepsilon_u(\mathrm{N})}{\varepsilon_m}$$

$$R_r = \frac{\varepsilon_u\,(\mathrm{N}) - \varepsilon_p\,(\mathrm{N})}{\varepsilon_u\,(N) - \varepsilon_p\,(N-1)}$$

All drug loaded films were cut dumbbell shape according to ISO 527-2 (type 5B) and immersed into sterilized PBS buffer (*p*H 7.4, *I* = 0.14 phosphate buffered solution (PBS)) in a vial (10 mL) with a dialyzed cap (MWCO = 10,000). Subsequently, the vial immersed into a bigger one containing 80 mL of the same release media and incubated at 37 °C. At each selected time point, 0.5 mL of PBS was collected for analysis and a fresh portion of PBS was added to continue the drug release experiment [27]. The concentration of released drug was measured with a UV-vis spectrometer at 229 nm.

Results and discussion

Characterization of SMP networks and drug- loaded films

In our previous work [30], a series of HPC-*g*-PCL-N prepolymers with different CL/HPC ratios and $Sn(Oct)_2$ catalyst amounts were prepared and cross-linked using various amounts of HDI to obtain X(HPC-*g*-PCL)-N networks. The detailed chemical structure of HPC-*g*-PCL prepolymers and networks is shown in Scheme S1 (Supporting Information). Among the prepared networks, the X(HPC-*g*-PCL)-90, X(HPC-*g*-PCL)-93 and X(HPC-*g*-PCL)-95 samples were selected for this study due to their high T_c (crystallization temperature) and X_c (degree of crystallinity) which are necessary to obtain good mechanical properties and SMP behavior. Furthermore, the X(HPC-*g*-PCL)-98 sample was prepared and studied due to its highest degree of crystallinity for comparison with aforementioned samples.

Figure S1 (Supporting Information) shows the FT-IR spectra of the prepared HPC-*g*-PCL-98 and X(HPC-*g*-PCL)-98 samples. The characteristic absorption peaks for the HPC-*g*-PCL-98 prepolymers were observed in the wave number region of ester carbonyl group stretching modes at 1726 cm^{-1}. Also, –OH group stretching mode at 3438 cm^{-1} attributed to the existence of terminal -OH of PCL. From the FT-IR spectrum of X(HPC-*g*-PCL), the crosslinking was confirmed by the presence of the new absorption bands corresponding to the N-H bending and stretching vibration of the urethane bonds appeared in 1580 and 3320 cm^{-1}, respectively. Also, the absorption peak of C=O in X(HPC-*g*-PCL) was slightly stronger and wider than the HPC-*g*-PCL due to the presence of carbamate and ester peaks [32]. Appearance of a new bond in 1620 cm^{-1} can be attributed to urea linkage which produced by a side reaction of H_2O with isocyanate groups, during the crosslinking procedure. It indicated successful crosslinking of prepolymers through terminal hydroxyl groups of PCL grafts and atmospheric H_2O by HDI. ^1H NMR spectrum of HPC-*g*-PCL-98 is shown in Fig. S2 (Supporting Information). As reported in previous research [30] the characteristic peaks of the HPC-*g*-PCL appeared as peaks a-e (Fig. S2, Supporting Information), approved the well synthesis of HPC-*g*-PCL-98.

In order to evaluate the effect of drug loading by different methods on polymer properties, naproxen as a well water-soluble drug at different loading levels was incorporated by in situ and swelling methods before and after crosslinking of HPC-*g*-PCL prepolymers, respectively. However, in spite of four samples prepared by the in situ method named: X(HPC-*g*-PCL)-95/3%, X(HPC-*g*-PCL)-95/10%, X(HPC-*g*-PCL)-98/3% and X(HPC-*g*-PCL)-98/10%, the samples prepared by the swelling method were unavoidably non-identical in terms of the drug content. The obtained results showed that naproxen loading in matrix of X(HPC-*g*-PCL)-95 and X(HPC-*g*-PCL)-98 polymers in order reached to 7.8 wt% and 12 wt% so they were named as X(HPC-*g*-PCL)-95/7.5% and X(HPC-*g*-PCL)-98/12%, respectively [12].

The values of gel content (G) and degree of swelling (Q) of the various X(HPC-*g*-PCL) and drug loaded-X(HPC-*g*-PCL) samples along with the calculated values of M_n for grafted PCL in corresponding precursor polymers are listed in

Table 1. The average length of the PCL segments (*L*) was estimated by ^{1}H NMR signals at $\delta = 3.64$ and 4.06 ppm, corresponding to the initial (I_{He}) and terminal ($I_{He'}$) methylene protons of the CL units, respectively (Fig. S2, Supporting Information). Based on this assignment, (L) could be calculated according to $L = I_{He}/I_{He'}$ [27].

As shown in Table 1, Q and G strongly depend on the molecular weight of PCL segment and content of loaded drug. Due to the high efficiency of curing through the crosslinking step, all systems present high values of G ranging from 92% to 99%. According to Table 1, as the chain length of PCL grafts decreases the number of grafting PCL chains increases, which led to an increase of the cross-link density. Also, by increasing PCL chain length the free volume in the polymer network became larger and its capacity to swell by more amount of solvent increased [33]. Similar finding was obtained for drug-loaded samples. As it is concluded from Table 1, in situ incorporation of drug into the polymer matrix, especially for high concentration of drug, are likely to disturb the crosslinking reaction. The resulting lower crosslinking densities could decrease G and increase Q compared to unloading drug state. Therefore, minimum values of G are belonged to drug loaded X(HPC-*g*-PCL)-95 with high amount of drug (10%). The obtained results for Q can be explained in the same way. Q has various data ranging from 10.2 for X(HPC-*g*-PCL)-95 to 28.18 for the drug loaded X(HPC-*g*-PCL)-98 sample due to the increasing of PCL chain length from 2451 to 5242. In this case, experimental data confirmed that drug loading reduces crosslink density and therefore led to greater swelling capability [32].

The thermal properties of synthesized prepolymers and networks were characterized using the DSC analysis. The curves obtained from the second DSC heating run for HPC-*g*-PCL prepolymers and X(HPC-*g*-PCL) films are shown in Fig. 1a and b, respectively. Their main thermal characteristic is summarized in Table S1 (Supporting Information). As it can be easily concluded from Table S1 (Supporting Information), decreasing of CL level leads to lower T_m and X_c. This result can be explained based on two reasons; the first is the amorphous nature of HPC that inhibited the crystal formation of grafted PCL chains via the incorporation HPC as a backbone. The second reason is the enhancement of overall number of active hydroxyl groups on the initiator by increasing the concentration of HPC. This can be resulted the lower length of PCL grafts as side chains. A notable decrease in T_m and X_c are observed upon network formation indicating that it has a strong influence on the degree of crystallinity via more limitation in mobility of PCL chains [27, 30, 32]. Also, in situ drug loaded networks show higher T_m, T_c and X_c than unloaded networks (Table 2) due to the interference of in situ drug loading by crosslinking reaction. The interaction of the naproxen carboxylic group with polycaprolactone hydroxyl groups in competition with diisocyanate molecules prevents chains chemically crosslinking reactions, which leads to lower crosslinking density and increases the degree of crystallinity of the network. However, in drug loaded networks by the swelling method, there is a significant reduction in these parameters for X(HPC-*g*-PCL)-95/7.8% and X(HPC-*g*-PCL)-98/12% networks, which evidently verify the networks morphological changes due to the drug incorporating (Fig. 1c and d). For further explanation, it can be attributed to the hydrogen bonds which resulted from the carboxylic group of naproxen with some of the hydroxyl groups of PCL which have been not participated in the crosslinking reaction. Consequently, this interaction slows down the polymeric chain movements, and ultimately reduces the degree of crystallinity of the polymeric network. On the other hand, naproxen as an impurity and a small molecule can place between polymeric chains, and inhibit polymer molecular movements. So, it reduces the degree of the crystallinity of PCL chains.

Figure 2a-d shows X-ray diffraction (XRD) patterns of the HPC-*g*-PCL prepolymers and their corresponding drug loaded and unloaded cross-linked films. As shown in Fig. 2a, the main diffraction peaks located at $2\theta = 21.56$ and 23.84° in agreement with those reported for PCL in the literature [30]. As seen in Table 2, the values of X_c, obtained from the XRD analysis are in well agreement with DSC results. These results suggest that the partially crystalline phase in the HPC-*g*-PCL originated from PCL side chains. Since the crystallinity strongly depends on PCL chains, the crystallinity of PCL side chains increases by increasing of their chain length. In accordance with the results of the DSC analysis, the intensity of crystalline diffraction peaks of PCL also decreased in crosslinked films (Fig. 2b). It can be interpreted based on the more amorphous nature of crosslinked films than their corresponding grafted copolymers.

Table 1 Gel content and degree of swelling of X(HPC-*g*-PCL) networks without and with drug loading

Sample	CL %	M_n of PCL segment on HPC repeating unit[a] (g/mol)	Gel content (%)	Degree of Swelling
X(HPC-*g*-PCL)-90	90	1261	99.65	6.34
X(HPC-*g*-PCL)-93	93	1759	99.37	6.48
X(HPC-*g*-PCL)-95	95	2700	99.26	10.02
X(HPC-*g*-PCL)-98	98	5405	98.85	12.21
X(HPC-*g*-PCL)-95/3% (In situ)	95	2700	96.47	14.63
X(HPC-*g*-PCL)-98/3% (In situ)	98	5405	98.13	22.17
X(HPC-*g*-PCL)-95/10% (In situ)	95	2700	92.00	16.92
X(HPC-*g*-PCL)-98/10% (In situ)	98	5405	96.33	28.18

[a] determined from ^{1}H NMR spectra

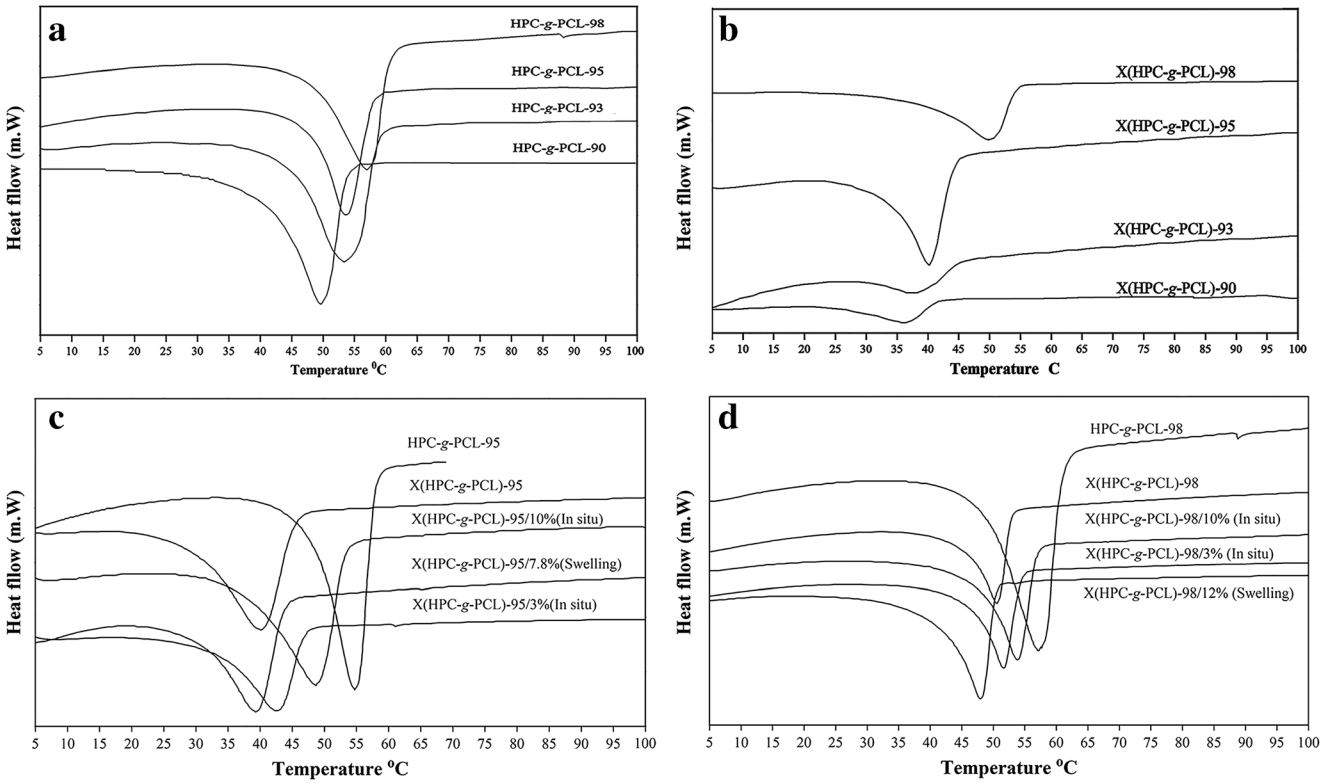

Fig. 1 DSC thermograms of HPC-*g*-PCL-90, −93, −95 and − 98 prepolymers (**a**), X(HPC-*g*-PCL)-90, −93, −95 and − 98 films (**b**), unloaded and drug loaded X(HPC-*g*-PCL)-95 films (**c**) and unloaded and drug loaded X(HPC-*g*-PCL)-98 films (**d**)

The degree of crystallinity of the crosslinked films is also affected by drug loading (Fig. 2c-d). According to Tables 1 and 2, as a consequence of the drug concentration enhancement, crosslink density is decreased and it caused significant increment in the -PCL crystallinity. In spite of drug loading via the in situ method, naproxen incorporation by the swelling method decrease the degree of crystallinity in the both X(HPC-*g*-PCL)-95 and X(HPC-*g*-PCL)-98 films. To explain the reason of this feature, as mentioned in previous section, it is suggested that the drug incorporation induced some changes in the network morphology and it decreased the PCL crystallinity. However, the results show the degree of crystallinity of the X(HPC-*g*-PCL)-95 is more affected by drug loading in compared to X(HPC-*g*-PCL)-98. The reason for this behavior can be probably interpreted that PCL chain length in X(HPC-*g*-PCL)-95 is shorter than X(HPC-*g*-PCL)-98. So, expect in the equal weights of both X(HPC-*g*-PCL)-95 and X(HPC-*g*-PCL)-98 networks, X(HPC-*g*-PCL)-95 have more hydroxyl groups, which can be led to the more chain-drug interactions. Consequently, X(HPC-*g*-PCL)-95 experiences more changes in its morphology than X(HPC-*g*-PCL)-95, and these more morphological changes will cause to more the degree of crystallinity reduction for X(HPC-*g*-PCL)-95 compared to X(HPC-*g*-PCL)-98.

The SEM micrographs represented in Fig. 3 show the cross-sectional view of the fracture surfaces of samples including the HPC-*g*-PCL-95 and HPC-*g*-PCL-98 prepolymers, their related crosslinked networks, and X(HPC-*g*-PCL)-98/3% and X(HPC-*g*-PCL)-98/12% drug loaded films via in situ and swelling methods, respectively. The SEM images verify

Table 2 Melting and crystallization temperatures, and degree of crystallinity of drug loaded X(HPC-*g*-PCL) films

Drug Loading method	X(HPC-*g*-PCL) drug loaded film	T_m (°C)[a]	T_c (°C)[b]	X_c (%)[c]	X_c (%)[d]
In situ	X(HPC-*g*-PCL)-95/3%	42.6	2.6	16.5	25
	X(HPC-*g*-PCL)-98/3%	51.6	28.1	22.8	34
	X(HPC-*g*-PCL)-95/10%	48.6	17.7	22.2	32
	X(HPC-*g*-PCL)-98/10%	53.7	29.1	30.7	48
Swelling	X(HPC-*g*-PCL)-95/7.8%	39.3	5.7	12.3	3
	X(HPC-*g*-PCL)-98/12%	47.9	20.3	21.9	26

[a,c] Obtained from second heating run in DSC analysis, [b] Obtained from cooling run in DSC analysis, [d] Obtained from XRD patterns

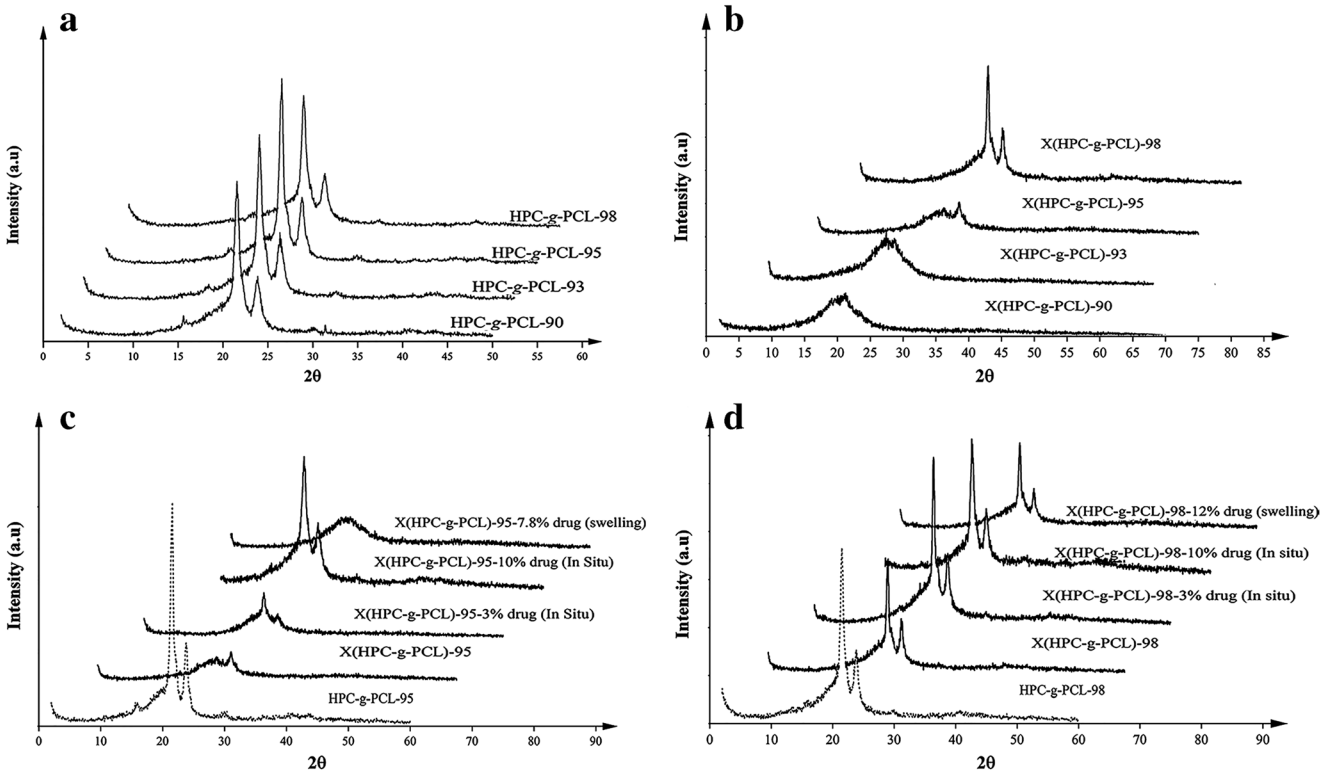

Fig. 2 XRD patterns of HPC-*g*-PCL-90, −93, −95 and − 98 prepolymers (**a**), X(HPC-*g*-PCL)-90, −93, −95 and − 98 films (**b**), unloaded and drug loaded X(HPC-*g*-PCL)-95 films (**c**) and unloaded and drug loaded X(HPC-*g*-PCL)-98 films (**d**)

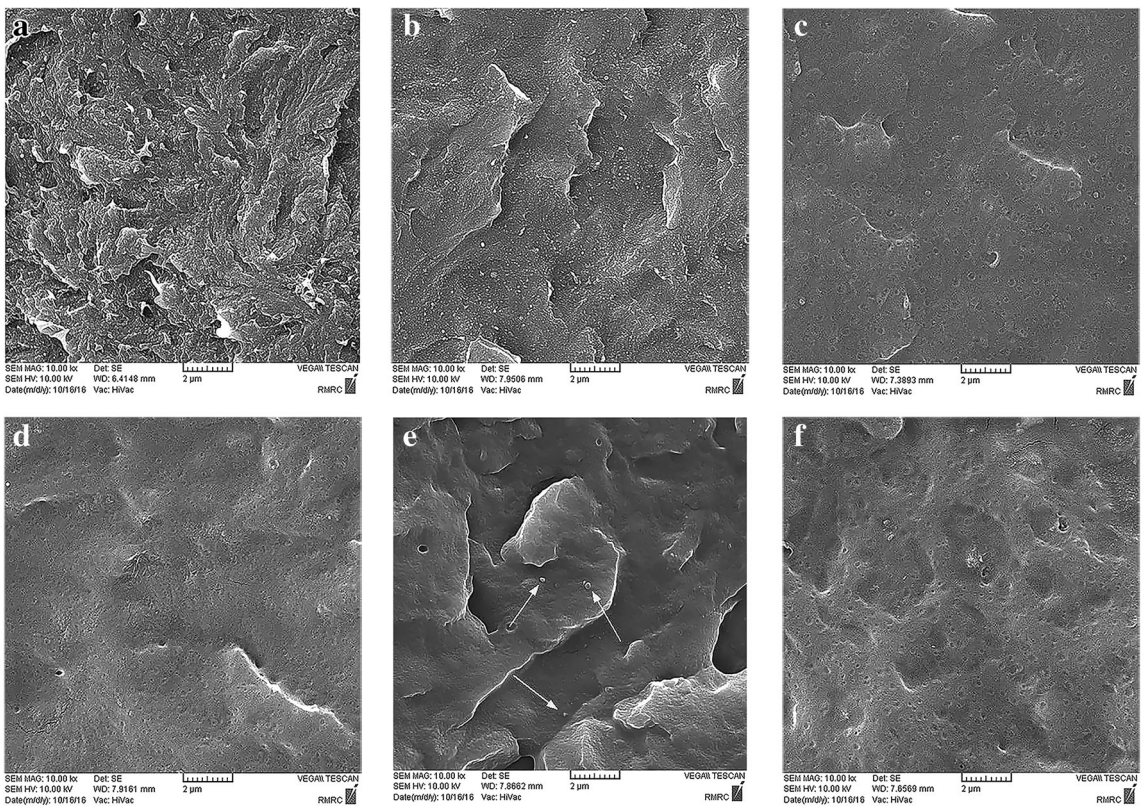

Fig. 3 SEM images of HPC-*g*-PCL-95 (**a**), HPC-*g*-PCL-98 prepolymers (**b**), X(HPC-*g*-PCL)-95 (**c**), X(HPC-*g*-PCL)-98 films(**d**), drug loaded X(HPC-*g*-PCL)-98/3% (In situ) (**e**) and X(HPC-*g*-PCL)-98/12% (swelling) (**f**)

the change of the HPC-*g*-PCL morphology after crosslinking and drug incorporation processes. A smooth ductile morphology was observed in both HPC-*g*-PCL-95 and 98 samples (Fig. 3a, b), whilst the brittle structure was seen for X(HPC-*g*-PCL)-95 and 98 (Fig. 3c, d) films. The morphological studies also supported the DSC and XRD results. As seen in Fig. 3e, the arrows marked presence of naproxen into the X(HPC-*g*-PCL)-98/3% (In situ). This sample shows smoother ductile fracture surfaces than the respected unloaded crosslinked network due to decrease of the crosslink density via the in situ naproxen loading method. On the other hand, drug loading by swelling (X(HPC-*g*-PCL)-98/12%) show more brittle fracture surfaces than the respected unloaded X(HPC-*g*-PCL)- 98 network (Fig. 3f).

Table S1 (Supporting Information) shows that T_m of X(HPC-*g*-PCL) films could be reduced to around body temperature by using of short PCL chains. Also, based on the DSC and XRD analyses, it could be concluded that X(HPC-*g*-PCL)-95 and X(HPC-g-PCL)-98 films may have suitable mechanical properties and the crystalline structure. Therefore, these films were chosen to undergo further analysis of the thermo-mechanical properties and shape memory effect. The mechanical properties of samples were evaluated from different points of view such as the effect of PCL graft chain length at different temperatures (22 °C, 37 °C and 65 °C), the influence of the drug loading method and the drug content of films. Young's modulus (E), elongation at break (ε_b %) and tensile strength (σ_m) of cross linked samples, obtained from tensile stress–strain curves, are summarized in Tables 2, 3, and 4. Figures 4a-b compare the mechanical properties of X(HPC-*g*-PCL)-95 and X(HPC-*g*-PCL)-98 samples at different temperatures (22 °C, 37 °C and 65 °C). The mechanical properties of the X(HPC-*g*-PCL)-98 film is significantly higher than the previously reported PCL-based SMP (Fig. 4b) [23, 27]. It is essential to recognize that thermo-mechanical properties affected by two important factors; the crystalline domains of the PCL chains and the crosslink density of network. The former acts as physical crosslinks and its effect is observed at lower temperature (22 °C), where both samples are at below their respective T_m and are partially crystalline. But, the latter has the more effect at high temperature (65 °C), because both samples are above their respective T_m and are completely amorphous. At 37 °C the samples show a partially crystalline nature which is an intermediate mode between the samples at 22 °C and the ones at 65 °C. Therefore, the E values are significantly controlled by crystallinity at low temperatures, but it is influenced by the crosslink density at higher temperatures. As shown in Table 3, by increasing of temperature, samples become much softer (lower E, and (σ_m)) and their mechanical properties decrease [23, 38]. According to the Tables 1 and 2, the longer PCL segment chain lengths, leads to the lower crosslink density and higher crystallinity. Hence, as observed in Table 3, at 22 °C the maximum and minimum values of E referred to X(HPC-*g*-PCL)-98 and X(HPC-*g*-PCL)-95 samples, respectively, while this order was completely inversed at 65 °C [21]. In addition, the mechanical properties of polymer networks containing drugs were determined by tensile test at 22 °C. Figures 4c-d depict the tensile curves in the unloaded and drug loaded states by two different loading methods of naproxen. According to Table 4, drug incorporation has no significant effect on σ_m and ε_b compared to the unloaded networks. On the other word, due to no change in the PCL chain length, both unloaded and drug loaded networks have almost the same σ_m and ε_b values. These results achieve while significant changes have been seen in Young's modulus after drug incorporation. While drug content reaches to 3% through the in situ method, a significant enhancement in Young's modulus can be seen for X(HPC-*g*-PCL)-98 and X(HPC-*g*-PCL)-95 samples (increasing from 376 to 528 MPa and from 143 to 326 MPa, respectivly). Further increase in naproxen content to 10% resulted less enhancement of E compared to their respective 3% drug loading samples. It should be related to the drug aggregation that cannot really affect well on the increasing the modulus. As expected, both X(HPC-*g*-PCL)-98 and X(HPC-*g*-PCL)-95 loaded networks by the swelling method exhibited a partially drop of E amount. This behavior could be resulted from changing morphology of network due to the drug incorporation.

According to Table 4, it is well seen that the entire drug loaded networks experienced a significantly reduction in their mechanical properties after the drug releasing procedure. This reduction in the mechanical properties can be related to the creation of some defects in polymer matrix during the drug releasing procedure. Briefly, it can be noted that morphological and not structural changes (crosslink density) during the swelling method lead to significant mechanical changes for

Table 3 Mechanical properties of X(HPC-*g*-PCL) films, measured at 22, 37 and 65 °C

X(HPC-*g*-PCL)-N	22 °C			37 °C			65 °C		
	E (MPa)	σ_m (MPa)	ε_b (%)	E (MPa)	σ_m (MPa)	ε_b (%)	E (MPa)	σ_m (MPa)	ε_b (%)
X(HPC-*g*-PCL)-95	143.0 ± 0.9	25.8 ± 0.3	128.2 ± 6.6	143.0 ± 0.5	36.56 ± 1.5	152.0 ± 8.6	24.4 ± 0.62	24.1 ± 1	89.4 ± 4.9
X(HPC-*g*-PCL)-98	376.0 ± 0.4	26.1 ± 1.0	324.0 ± 8.5	322.0 ± 0.1	37.12 ± 0.8	222.9 ± 5.4	11.2 ± 0.3	39.7 ± 0.3	286.1 ± 12

Each test was conducted for at least three specimens and was repeated three times

Table 4 The effect of drug content, loading method and release of the drug on thermo-mechanical properties of X(HPC-*g*-PCL) films, measured at 22 °C

X(HPC-*g*-PCL)-N	E (MPa)	σ_m (MPa)	ε_b %
X(HPC-*g*-PCL)-95	143.0 ± 0.9	25.8 ± 0.3	128.2 ± 6.6
X(HPC-*g*-PCL)-98	376.0 ± 0.4	26.1 ± 1.0	324.0 ± 8.5
X(HPC-*g*-PCL)-95/3% (In situ)	326.0 ± 4.5	23.0 ± 2.7	129.0 ± 9.6
X(HPC-*g*-PCL)-98/3% (In situ)	528.0 ± 3.8	29.0 ± 1.3	356.0 ± 7.7
X(HPC-*g*-PCL)-95/3% (In situ)[a]	72.5 ± 2.9	21.2 ± 1.4	65.2 ± 4.9
X(HPC-*g*-PCL)-98/3% (In situ)[a]	524.5 ± 3.6	22.7 ± 1.2	248.6 ± 5.5
X(HPC-*g*-PCL)-95/10% (In situ)	268.1 ± 1.1	23.5 ± 0.7	116.0 ± 5.1
X(HPC-*g*-PCL)-98/10% (In situ)	327.9 ± 1.8	18.4 ± 2.1	28.5 ± 2.9
X(HPC-*g*-PCL)-95/7.8% (Swelling)	102.0 ± 0.9	28.0 ± 1.3	140.0 ± 3.6
X(HPC-*g*-PCL)-98/12% (Swelling)	345.0 ± 1.7	31.0 ± 2.6	310.0 ± 4.8
X(HPC-*g*-PCL)-95/7.8% (Swelling)[a]	324.2 ± 3.1	25.8 ± 1.9	94.4 ± 4.8
X(HPC-*g*-PCL)-98/12% (Swelling)[a]	389.0 ± 2.9	18.0 ± 2.5	121.9 ± 3.4

Each test was conducted for at least three specimens and was repeated three times

[a] After drug releasing procedure

this type of films after drug release than the one loaded via the in situ method. Although the incorporation of drug into the polymer matrix decreases some mechanical properties, it could not distinctly influence the application of the materials in the biomedical field [39].

The thermally induced shape-memory behavior of X(HPC-*g*-PCL)-N films is shown in Fig. 5a-d . To the best of our knowledge, shape recovery is mostly affected by cross-linking density while shape fixity is influenced by crystallinity of the switching segments in networks. The shape-recovery (R_r), and shape fixity (R_f) of unloaded and drug loaded X(HPC-*g*-PCL)-95 and X(HPC-*g*-PCL)-98 films were measured by thermo-mechanical tensile experiments and the results are listed in Tables 5 and 6. During the test, the samples

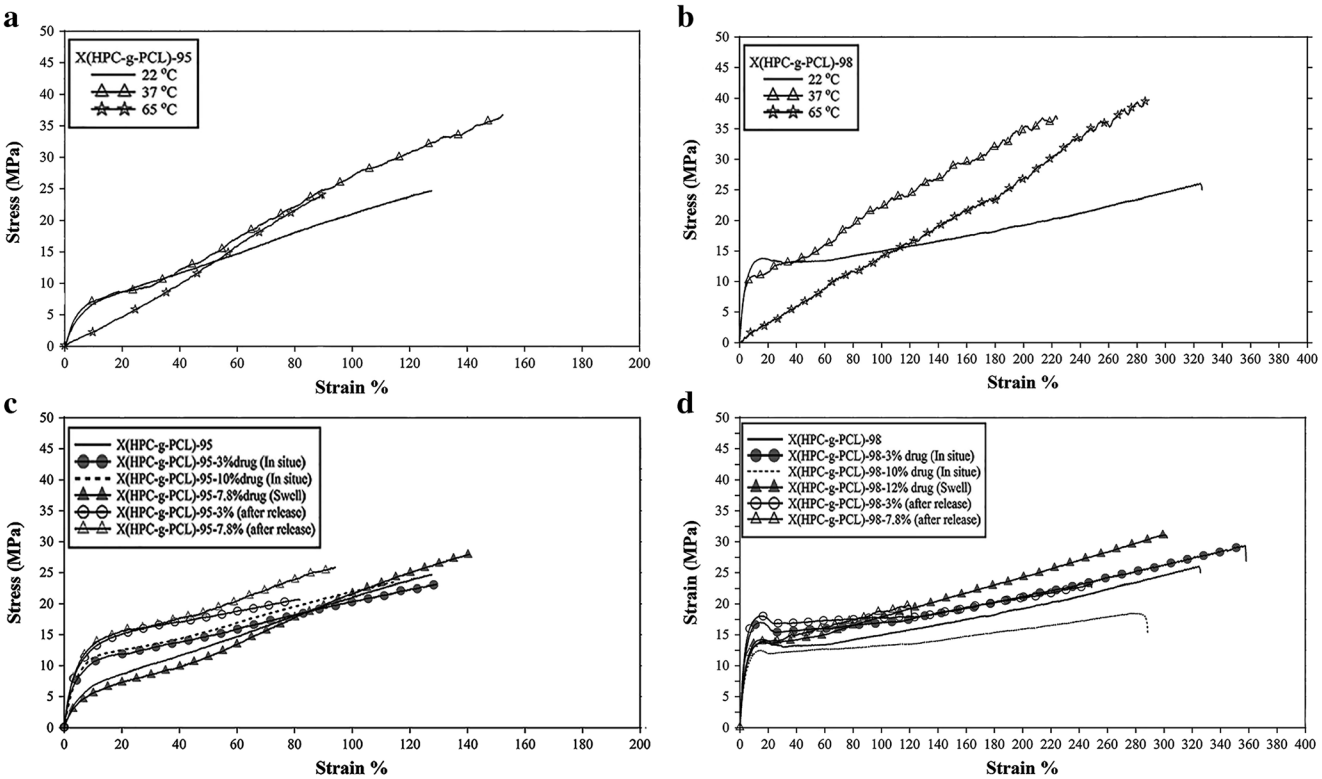

Fig. 4 Stress-strain curves of X(HPC-*g*-PCL)-95 films at 22, 37 and 65 °C (a), X(HPC-*g*-PCL)-98 films at 22, 37 and 65 °C (b), X(HPC-*g*-PCL)-95 drug loaded and unloaded films at 22 °C (c), X(HPC-*g*-PCL)-98 drug loaded and unloaded films at 22 °C (d)

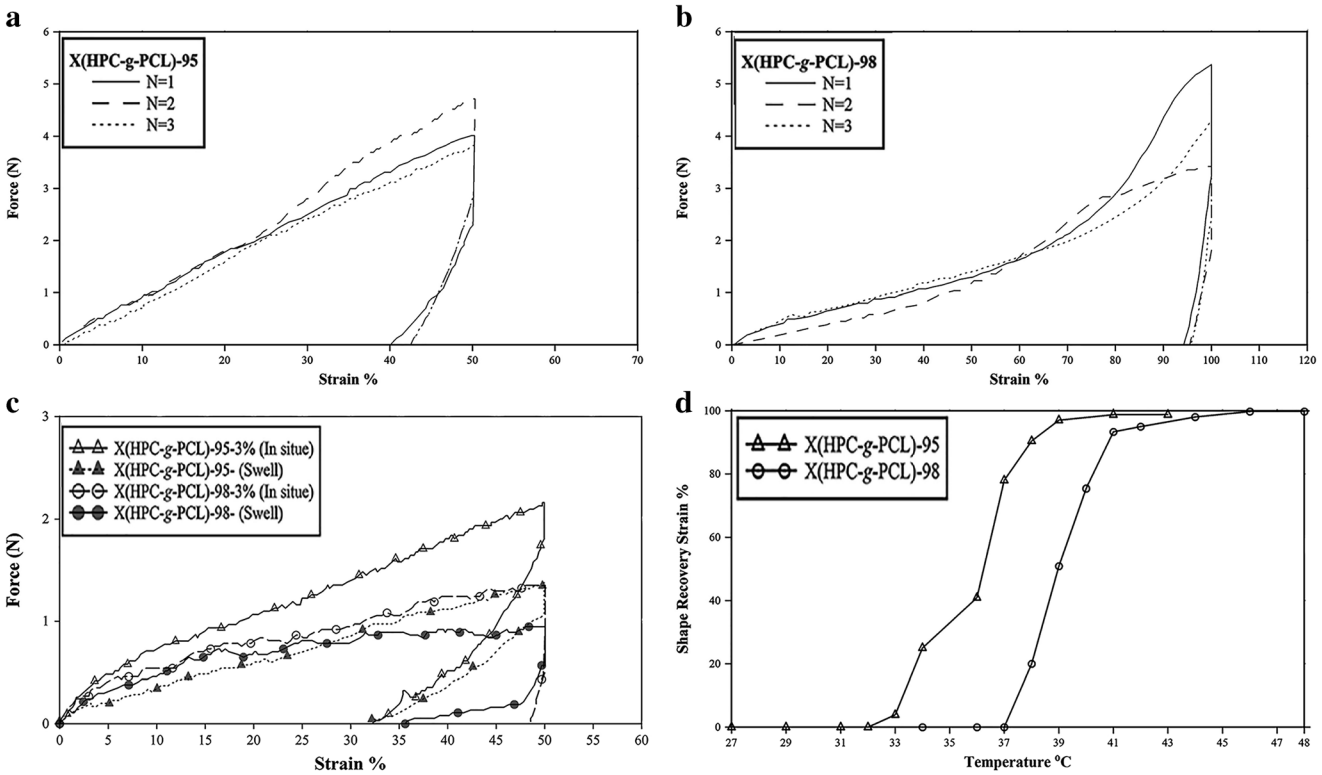

Fig. 5 Force–strain curves obtained from thermo-mechanical tests with initial deformation at room temperature for unloded X(HPC-*g*-PCL)-95 films (**a**), unloaded X(HPC-*g*-PCL)-98 films (**b**), drug loaded X(HPC-*g*-PCL)-95 and X(HPC-*g*-PCL)-98 films after drug releasing (**c**), Shape recovery ratio vs. temperature for unloaded X(HPC-*g*-PCL)-95 and X(HPC-*g*-PCL)-98 films in water (**d**)

were first elongated at 65 °C to a certain strain (ε_m) of 50% (for the X(HPC-*g*-PCL)-95 film) (Fig. 5a) or 100% (for the X(HPC-*g*-PCL)-98 film) (Fig. 5b), by applying a constant elongation rate of 5 mm/min. Temporary shape was fixed by cooling the samples to 22 °C at the same constant strain, then unloaded strain (εu) was correspondingly recorded. Subsequently, shape recovery was determined upon heating the samples up to their corresponding T_m and ε_p was recorded. This completed thermo-mechanical cycle ($N = 1$), and three additional cycles were carried out using the same method [19, 37, 40, 41]. The shape-memory behavior for X(HPC-*g*-PCL) networks was clearly observed. By considering almost fully crosslinking of all unloaded HPC-*g*-PCL polymers (Table 1), both X(HPC-*g*-PCL)-98 and X(HPC-*g*-PCL)-95 samples exhibited excellent shape recovery (R_r) values even after 3 cycles, which were reliably higher than 95%. [32, 42]. The R_r values are relatively low in the first cycle, but exceeded to 99% after 3 cycles. Although, molecular weight and crystallinity of PCL segments have only a negligible effect on R_r, their effects on R_f are quite obvious. The R_f value was increased by increasing of molecular weight of the PCL side chain. Increasing the crystallinity of the PCL side chain causes the material to be able to hold inner stress to preserve temporary shape. Hence, as seen in Table 5, the X(HPC-*g*-PCL)-98 sample with the high degree of crystallinity content of PCL side chain exhibits higher value of shape fixity than X(HPC-*g*-PCL)-95 sample [19, 32].

Shape memory behavior of X(HPC-*g*-PCL)-95 and X(HPC-*g*-PCL)-98 films was also investigated after drug releasing. For this purpose, all samples were elongated up to 50% of their original length under the same condition which previously described for unloaded samples. The results are summarized in Table 6. As seen in Fig. 5c, R_f values have been significantly

Table 5 Shape fixity, shape recovery, and transition temperature of X(HPC-*g*-PCL) films at different thermo-mechanical test cycles

Samples	Shape fixity (%)			Shape recovery (%)			Recovery temperature (°C)
	N(1)	*N*(2)	*N*(3)	*N*(1)	*N*(2)	*N*(3)	
X(HPC-*g*-PCL)-95	80 ± 0.86	84 ± 0.09	84 ± 0.28	95.7 ± 0.56	97.3 ± 0.88	98.8 ± 0.39	33–39
X(HPC-*g*-PCL)-98	96 ± 0.42	95 ± 1.13	96 ± 0.18	96.7 ± 1.34	98.4 ± 0.95	99.4 ± 1.25	38–41

Each test was conducted for at least three specimens and was repeated three times

Table 6 Shape fixity, shape recovery, and transition temperature of drug loaded X(HPC-*g*-PCL) films after drug releasing

Samples	Unloaded films		Drug loaded films (In situ 3%) After drug releasing		Drug loaded films (swelling) After drug releasing	
	R_f%	R_r%	R_f%	R_r%	R_f%	R_r%
X(HPC-*g*-PCL)-95	80.0 ± 0.86	95.7 ± 0.56	63.0 ± 0.06	86.6 ± 1.1	62.0 ± 2.1	96.8 ± 0.3
X(HPC-*g*-PCL)-98	95.0 ± 0.42	96.7 ± 1.34	95.0 ± 0.70	89.0 ± 1.3	72.0 ± 0.8	97.4 ± 1.1

Each test was conducted for at least three specimens and was repeated three times

decreased by reducing the crystallinity of PCL side chains. Low crystallinity causes the PCL chains not to be able to preserve the internal stress to maintain the temporary shape [32].

As seen in Tables 2, 3%*w*/w naproxen loading into the polymer matrix through the in situ method did not affect significantly on the crystallinity of the X(HPC-*g*-PCL)-98 network. Therefore, in situ drug-loaded (after drug releasing) networks as well as unloaded polymer ones show comparable shape fixity (Table 5). As expected, the swelling incorporation method allows further morphological changes and subsequent reduction of networks crystallinity. Thereby, the swelling incorporation of naproxen reduces R_f as was observed in Table 5. For instance, the differences of shape fixity for unloaded X(HPC-*g*-PCL)-98 and loaded X(HPC-*g*-PCL)-98 after drug releasing was significant. R_f in X(HPC-g-PCL)-98 drug loaded by swelling experienced a decrease of 23% after drug releasing)R_f = 72%). The results showed drug releasing from X(HPC-g-PCL)-95, which loaded by both drug incorporation methods, led to evidently reduction of R_f.

As mentioned before, the in situ drug loading method reduces the networks crosslinking density and both X(HPC-*g*-PCL)-95 and X(HPC-*g*-PCL)-98 samples exhibited lower R_r compared to unloaded films. However, both X(HPC-*g*-PCL)-95 and X(HPC-*g*-PCL)-98 samples, which drug loaded by the swelling method, kept their shape recoverability in comparison with the corresponding unloaded networks. These results confirmed that the drug loading by the swelling method have no influence on the networks crosslinking density.

Strain recovery curves of the X(HPC-*g*-PCL)-95 and X(HPC-*g*-PCL)-98 samples as a function of temperature was conducted in water according to the description follow and the results are shown in Fig. 5d. First, the samples were elongated up to 200% of their original length in 65 °C hot water. Then cooled down below their melting point (fixing the temporary shape) and, eventually, it placed into a 20 °C water bath and warmed in a rate of 1 °C per minute (till 39 °C). As seen in Fig. 5d, both the measured curves are S-shaped, and T_{trans} for X(HPC-*g*-PCL)-95 and X(HPC-*g*-PC)-98 are around 36 and 41 °C, respectively. The T_{trans} of both networks are significantly lower than their T_m, and are in a good agreement with the melting onset point on the corresponding DSC thermograms.

Shape memory behavior of X(HPC-*g*-PCL) is demonstrated in Fig. 6a-c. X(HPC-*g*-PCL) in its permanent shape (6a) was heated at 55 °C and kept for 2 min. The sample was deformed into its temporary shape and cooled into a 0 °C ice water bath for freezing the stress and fixing into the temporary shape for 1 min (6b) [42]. Eventually, it placed into a 20 °C water bath and warmed in a rate of 1 °C per minute. When the water bath temperature reached to 39 °C the deformed sample come back to its permanent shape just in 10s (6c).

In vitro naproxen release behavior

Drug-loaded SMP films were prepared using naproxen as a conventional model drug. Figure 7 shows cumulative profiles of naproxen release from X(HPC-*g*-PCL)-95 and X(HPC-*g*-PCL)-98 films which loaded by two different methods. Figure 7a-c exhibit drug release profiles of X(HPC-*g*-PCL)-95/3%, (In situ) and X(HPC-*g*-PCL)-98/3% (In situ) (a); X(HPC-*g*-PCL)-95/10% (In situ) and X(HPC-*g*-PCL)-98/10% (In situ) (b); and X(HPC-*g*-PCL)-95/7.8% (Swelling) and X(HPC-*g*-PCL)-98/12% (Swelling) (c) films. As seen in Fig. 7, the release curves are basically identical for all samples. Results show that the initial release of the drug depends on the amount of the loaded drug, so higher amount of loaded drug leads to greater initial release. In both (a) and (b) films, regardless of the amount of loaded drug, it is clearly seen that the initial release of the drug from X(HPC-*g*-PCL)-95 is more than the X(HPC-*g*-PCL)-98. It can be attributed to the higher degree of entanglement in X(HPC-*g*-PCL)-98 chains, due to its longer chain length, which resulted to more trapping drug and more slowly rate of releasing [27, 29, 38, 40–44]. Drug release profile of (c) films showed two importance differences than the in situ method: (i) a burst initial release was seen for both network due to dominate surface adsorption of swelling compared to the in situ method; (ii) the initial release of the drug from X(HPC-*g*-PCL)-95 is less than the X(HPC-*g*-PCL)-98. This result can be related to more swelling degree for X(HPC-*g*-PCL)-98 than X(HPC-*g*-PCL)-95 which led to more drug incorporated into X(HPC-*g*-PCL)-98 compared to X(HPC-*g*-PCL)-95. On the other side, inherently PCL is a hydrophobic polymer, so it is reasonable that PCL chains experiences no swelling in water as a drug releasing medium. Hence, in this study, the drug releasing rate is independent from network swelling degree, but related to the amount of drug loading and the chain entanglements.

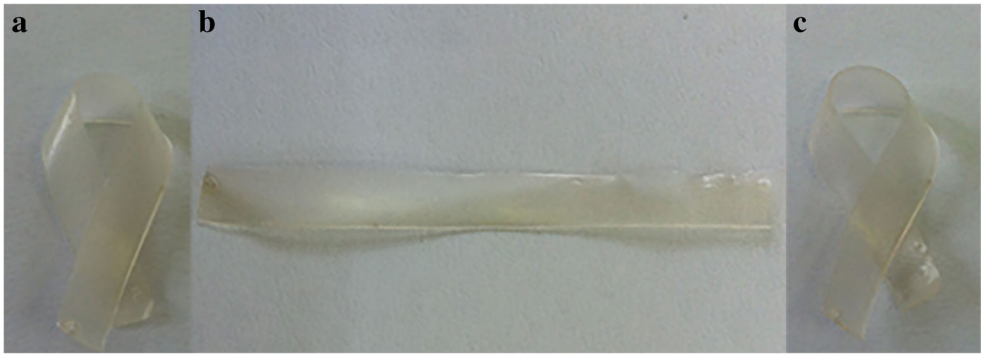

Fig. 6 Thermally induced shape-memory behavior of X(HPC-*g*-PCL) SMP films (with 4.8 cm length and 0.1 mm thickness) (**a**) Permanent shape (**b**) temporary shape fixed at o °C (**c**) the recovered shape after 10 s immersion in water at 39 °C

Below a temperature of 37 °C, no significant UV absorption of naproxen was obtained after the burst initial release for both in situ and swelling drug loaded networks. It is a strong reason for the thermo-sensitivity of the X(HPC-g-PCL) polymer for the controlled drug release.

Conclusion

In summary, a series of PCL-based network polymers X(HPC-g-PCL) were prepared via ring opening polymerization of CL by HPC and then were chemically cross-linked the PCL side chains in excellent yields. Obtained networks were characterized in terms of their gel content, degree of swelling, melting temperature, degree of crystallinity, and morphology. The degree of crystallinity and the melting temperature of resulted cross-linked polymers were affected by altering the molecular weight of PCL side chains. The results of DSC and XRD analyses showed that the crystalline structure of the X(HPC-*g*-PCL) sample originated from PCL side chains and related to CL/HPC ratio in the reaction feed. Among synthesized samples, X(HPC-*g*-PCL)-95 and − 98 films satisfy thermo-mechanical properties with combining shape memory effect. The results showed that the mechanical properties significantly depend on the polycaprolactone chains length. On the other hand, the amount of loaded drug and the type of the loading method caused significant effects on mechanical properties. The X(HPC-*g*-PCL)-98 sample with higher molecular weight of PCL showed high shape recovery behavior by a narrower recovery temperature ranging from 39 to 41 °C as well as higher shape fixity than the X(HPC-*g*-PCL)-95 sample. As a result, by tailoring the graft copolymer architecture precisely, shape-memory switching temperatures could be successfully adjusted near body temperature while retaining a sharp transition in a narrow temperature range. X(HPC-*g*-PCL)-95 and − 98 samples as drug-loaded shape memory polymers were successfully prepared by introducing naproxen as a model drug through two different drug loading methods (loading by swelling and in situ methods). Drug loading by the swelling method is typically introduced a non-controllable loading levels with burst initial release depending on the drugs physicochemical properties. Besides, the in situ loading method related to controllable drug payload and resulted in lower burst and higher subsequent release. Despite the initial release which depends on the initial amount of the incorporated drug, network capacity and chain entanglements, both drug loading methods showed the same release profiles. X(HPC-*g*-PCL)-95 and − 98 samples' thermo-

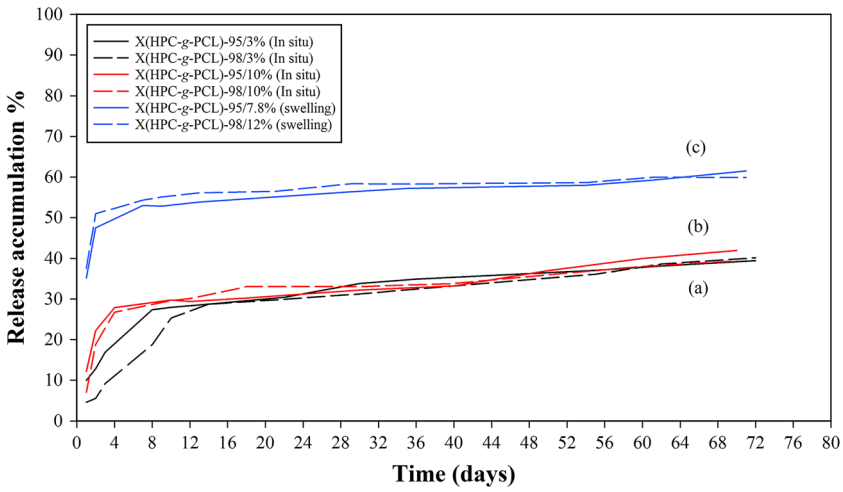

Fig. 7 In vitro release profile of naproxen from X(HPC-*g*-PCL)-95/3%, (In situ), X(HPC-*g*-PCL)-98/3% (In situ) (a), X(HPC-*g*-PCL)-95/10% (In situ), X(HPC-*g*-PCL)-98/10% (In situ) (b), and X(HPC-*g*-PCL)-95/7.8% (Swelling) and X(HPC-*g*-PCL)-98/12% (Swelling) films in PBS at 37 °C

mechanical properties and shape memory effect decreased after the sustained drug release over 70 days, but their ability to use in medical applications is debatable. Therefore, HPC-*g*-PCL networks could be introduced as SMPs with T_{trans} relatively higher than the body temperature (39–41 °C), excellent mechanical properties, shape fixing potential, shape recovery and drug release capability to make a promising system for biomedical applications.

Acknowledgements We thank the Vice Chancellor of Research of Azarbaijan Shahid Madani University, for financially supporting this research.

References

1. Hu J, Meng H, Li G, Ibekwe SI (2012) A review of stimuli-responsive polymers for smart textile applications. Smart Mater Struct 21:053001
2. Chan BQ, Low ZW, Heng SJ, Chan SY, Owh C, Loh XJ (2016) Recent advances in shape memory soft materials for biomedical applications. ACS Appl Mater Inter 8:10070–10087
3. Heuchel M, Sauter T, Kratz K, Lendlein A (2013) Thermally induced shape-memory effects in polymers: quantification and related modeling approaches. J Polym Sci Pol Phys 51:621–637
4. Zhang H, Xia H, Zhao Y (2014) Light-controlled complex deformation and motion of shape-memory polymers using a temperature gradient. ACS Macro Lett 3:940–943
5. Chen H, Li Y, Liu Y, Gong T, Wang L, Zhou S (2014) Highly pH-sensitive polyurethane exhibiting shape memory and drug release. Polym Chem 5:5168–5174
6. Du H, Zhang J (2010) Solvent induced shape recovery of shape memory polymer based on chemically cross-linked poly (vinyl alcohol). Soft Matter 6:3370–3376
7. Kumpfer JR, Rowan SJ (2011) Thermo-, photo-, and chemo-responsive shape-memory properties from photo-cross-linked metallo-supramolecular polymers. J Am Chem Soc 133:12866–12874
8. Du FP, Ye EZ, Yang W, Shen TH, Tang CY, Xie XL, Zhou XP, Law WC (2015) Electroactive shape memory polymer based on optimized multi-walled carbon nanotubes/polyvinyl alcohol nanocomposites. Compos Part B-Eng 68:170–175
9. Bai S, Zou H, Dietsch H, Simon YC, Weder C (2014) Functional Iron oxide nanoparticles as reversible crosslinks for magnetically addressable shape-memory polymers. Macromol Chem Physic 215:398–404
10. Ward Small IV, Singhal P, Wilson TS, Maitland DJ (2010) Biomedical applications of thermally activated shape memory polymers. J Mater Chem 20:3356–3366
11. Leng J, Lan X, Liu Y, Du S (2011) Shape-memory polymers and their composites: stimulus methods and applications. Prog Mater Sci 56:1077–1135
12. Neffe AT, Hanh BD, Steuer S, Lendlein A (2009) Polymer networks combining controlled drug release, biodegradation, and shape memory capability. Adv Mater 21:3394–3398
13. Tan L, Gan L, Hu J, Zhu Y, Han J (2015) Functional shape memory composite nanofibers with graphene oxide filler. Compos Part A-Appl Sci 76:115–123
14. Ebara M (2015) Shape-memory surfaces for cell mechanobiology. Sci Tchnol Adv Mat 16:014804
15. Wong Y, Kong J, Widjaja LK, Venkatraman SS (2014) Biomedical applications of shape-memory polymers: how practically useful are they? Sci China Chem 57:476–489
16. Bobel AC, McHugh PE (2018) Computational analysis of the utilisation of the shape memory effect and balloon expansion in fully polymeric stent deployment. Cardiovasc Eng Techn 9:60–72
17. Serrano MC, Ameer GA (2012) Recent insights into the biomedical applications of shape-memory polymers. Macromol Biosci 12:1156–1171
18. Ebara M, Uto K, Idota N, Hoffman JM, Aoyagi T (2014) Shape-memory surface with dynamically tunable Nano-geometry activated by body heat. Adv Mater 26:358–358
19. Xue L, Dai S, Li Z (2009) Synthesis and characterization of three-arm poly (ε-caprolactone)-based poly (ester− urethanes) with shape-memory effect at body temperature. Macromolecules. 42:964–972
20. El Feninat F, Laroche G, Fiset M, Mantovani D (2002) Shape memory materials for biomedical applications. Adv Eng Mater 4:91–104
21. Wischke C, Neffe AT, Steuer S, Lendlein A (2009) Evaluation of a degradable shape-memory polymer network as matrix for controlled drug release. J Control Release 138:243–250
22. Niu Y, Zhang P, Zhang J, Xiao L, Yang K, Wang Y (2012) Poly (p-dioxanone)–poly (ethylene glycol) network: synthesis, characterization, and its shape memory effect. Polym Chem 3:2508–2516
23. Le DM (2012) Advances in the synthesis and application of polycaprolactone shape memory polymer biomaterials. PhD Dissertation, University of North Carolina at Chapel Hill
24. Zhang D, Petersen KM, Grunlan MA (2012) Inorganic–organic shape memory polymer (SMP) foams with highly tunable properties. ACS Appl Mater Inter 5:186–191
25. Meng Y, Jiang J, Anthamatten M (2016) Body temperature triggered shape-memory polymers with high elastic energy storage capacity. J Polym Sci Pol Phys 54:1397–1404
26. Basfar AA, Lotfy S (2015) Radiation-crosslinking of shape memory polymers based on poly (vinyl alcohol) in the presence of carbon nanotubes. Radiat Phys Chem 106:376–384
27. Nagahama K, Ueda Y, Ouchi T, Ohya Y (2009) Biodegradable shape-memory polymers exhibiting sharp thermal transitions and controlled drug release. Biomacromolecules. 10:1789–1794
28. Alteheld A, Feng Y, Kelch S, Lendlein A (2005) Biodegradable, amorphous copolyester-urethane networks having shape-memory properties. Angew Chem Int Edit 44:1188–1192
29. Serrano MC, Carbajal L, Ameer GA (2011) Novel biodegradable shape-memory elastomers with drug-releasing capabilities. Adv Mater 23:2211–2215
30. Jahangiri M, Bagheri M, Farshi F, Abbasi F (2015) Optimized synthesis of hydroxypropyl cellulose-g-poly (ε-caprolactone) network. J Polym Res 22:196
31. Shi R, Burt HM (2003) Synthesis and characterization of amphiphilic hydroxypropylcellulose-graft-poly (ε-caprolactone). J Appl Polym Sci 89:718–727
32. Bai Y, Jiang C, Wang Q, Wang T (2013) A novel high mechanical strength shape memory polymer based on ethyl cellulose and polycaprolactone. Carbohyd Polym 96:522–527
33. Pandini S, Baldi F, Paderni K, Messori M, Toselli M, Pilati F, Gianoncelli A, Brisotto M, Bontempi E, Ricco T (2013) One-way and two-way shape memory behaviour of semi-crystalline networks based on sol–gel cross-linked poly (ε-caprolactone). Polymer 54:4253–4265
34. Chen S, Mo F, Yang Y, Stadler FJ, Chen S, Yang H, Ge Z (2015) Development of zwitterionic polyurethanes with multi-shape memory effects and self-healing properties. J Mater Chem A 3:2924–2933
35. Gaj MP, Wei A, Fuentes-Hernandez C, Zhang Y, Reit R, Voit W, Marder SR, Kippelen B (2015) Organic light-emitting diodes on

shape memory polymer substrates for wearable electronics. Org Electron 25:151–155
36. Kalajahi AE, Rezaei M, Abbasi F (2016) Preparation, characterization, and thermo-mechanical properties of poly (ε-caprolactone)-piperazine-based polyurethane-urea shape memory polymers. J Mater Sci 51:4379–4389
37. Hu J, Yang Z, Yeung L, Ji F, Liu Y (2005) Crosslinked polyurethanes with shape memory properties. Polym Int 54:854–859
38. Wischke C, Neffe AT, Steuer S, Lendlein A (2010) Comparing techniques for drug loading of shape-memory polymer networks–effect on their functionalities. Eur J Pharm Sci 41:136–147
39. Yu X, Shaobing Z, Lin W (2010) Crosslinked poly (e-Caprolactone)/poly (Sebacic anhydride) compo-sites combining biodegradation, controlled drug release and shape memory effect. Compos Part B-Eng 41:537–542
40. Xue L, Dai S, Li Z (2012) Synthesis and characterization of elastic star shape-memory polymers as self-expandable drug-eluting stents. J Mater Chem 22:7403–7411
41. Peponi L, Navarro-Baena I, Sonseca A, Gimenez E, Marcos-Fernandez A, Kenny JM (2013) Synthesis and characterization of PCL–PLLA polyurethane with shape memory behavior. Eur Polym J 49:893–903
42. Wang L, Di S, Wang W, Chen H, Yang X, Gong T, Zhou S (2014) Tunable temperature memory effect of photo-cross-linked star PCL–PEG networks. Macromolecules 47:1828–1836
43. Mya KY, Gose HB, Pretsch T, Bothe M, He C (2011) Star-shaped POSS-polycaprolactone polyurethanes and their shape memory performance. J Mater Chem 21:4827–4836
44. Li G, Fei G, Xia H, Han J, Zhao Y (2012) Spatial and temporal control of shape memory polymers and simultaneous drug release using high intensity focused ultrasound. J Mater Chem 22:7692–7696